Journal of Colloid and Interface Science 572 (2020) 374–383

Contents lists available at ScienceDirect

Journal of Colloid and Interface Science

journal homepage: www.elsevier.com/locate/jcis

Band bending of TiO_2 induced by O-xylene and acetaldehyde adsorption and its effect on the generation of active radicals

Qinglong Zeng [a,b], Xiao Wang [a], Xiaofeng Xie [a,*], Asad Mahmood [a], Guanhong Lu [a], Yan Wang [a], Jing Sun [a,*]

[a] State Key Lab of High Performance Ceramics and Superfine Microstructure, Shanghai Institute of Ceramics, Chinese Academy of Sciences, 1295 Dingxi Road, Shanghai 200050, China
[b] University of Chinese Academy of Sciences, 19 Yuquan Road, Beijing 100049, China

HIGHLIGHTS

- O-xylene and acetaldehyde adsorption could influence the band structure of TiO_2.
- O-xylene was acceptor molecule while acetaldehyde was donor molecule.
- Acetaldehyde and o-xylene adsorption would change the band structure of TiO_2.
- The photocatalysis of o-xylene was dominant by $^{\cdot}OH$, while the photocatalysis of acetaldehyde was dominant by $^{\cdot}O_2^-$.

GRAPHICAL ABSTRACT

Different band bending situations would be formed when o-xylene and acetaldehyde adsorbed on TiO_2 surface, and this could result in different generation situations of active radicals.

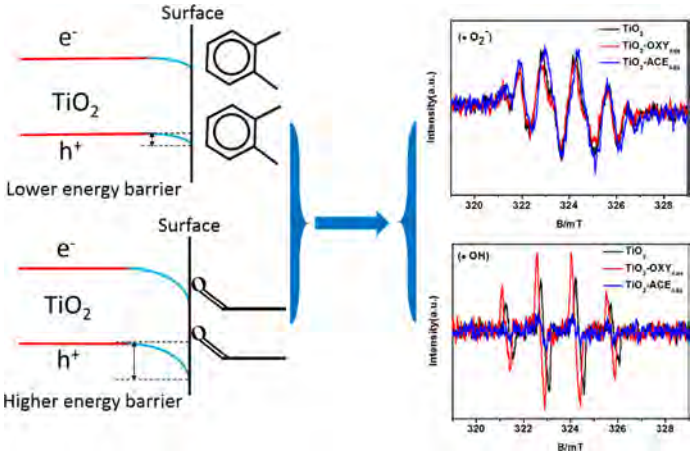

ARTICLE INFO

Article history:
Received 1 February 2020
Revised 26 March 2020
Accepted 29 March 2020
Available online 31 March 2020

Keywords:
Sol-gel method
Band bending
O-xylene
Acetaldehyde
Active radicals
Photocatalysis

ABSTRACT

Most studies on the photodegradation of volatile organic compounds (VOCs) have focused on the synthesis of efficient photocatalysts. However, little attention has been paid to the band bending change of semiconductive photocatalysts after the adsorption of VOCs. Herein, we first disclose how the adsorption of two typical VOCs influences the band bending of P-type rutile TiO_2 and consequently changes the amount of reactive radicals. This provides a new way to understand the experimental phenomenon of heterogeneous reactions. Theoretical computations of the adsorption model and zeta potential tests both verified that o-xylene is an acceptor molecule when it adsorbs on the TiO_2 surface, and it tends to attract electrons from TiO_2. In contrast, acetaldehyde is a donor molecule. A distinct electron transfer direction between TiO_2 and adsorbed molecules (o-xylene and acetaldehyde) induces a different band bending degree. O-xylene adsorption alleviates the downward band bending of TiO_2 itself, whereas acetaldehyde adsorption strengthens the downward band bending. The probability of electrons and holes reaching the TiO_2 surface is influenced by this change, which has a considerable influence on the generation of active radicals. Consequently, o-xylene adsorption leads to more hydroxyl radical generation, and acetaldehyde adsorption results in less hydroxyl radical generation. As a result, hydroxyl radicals play the predominant role in the degradation of o-xylene, whereas the photocatalysis of acetaldehyde is dominant for

* Corresponding authors.
E-mail addresses: xxfshcn@163.com (X. Xie), jingsun@mail.sic.ac.cn (J. Sun).

https://doi.org/10.1016/j.jcis.2020.03.114

superoxide radicals. In addition, the band bending of a semiconductor induced by gaseous molecule adsorption has the potential for application in gas sensors to improve sensitivity.

1. Introduction

O-xylene and acetaldehyde are two typical volatile organic compounds (VOCs) that have attracted much attention [1–6]. These VOCs are very common contaminants in our daily life, including in indoor and outdoor environments, and they are harmful to human health [7–10]. It is crucial to remove them from our living environments. For the elimination of VOCs, photocatalysis is one of the most effective treatments. TiO_2 is one of the most popular photocatalysts because of its non-toxicity, low price, abundance, and good stability [11–19]. Although TiO_2 has many advantages, some challenges still exist when it is applied for the photodegradation of o-xylene and acetaldehyde. Three main drawbacks limit the application of TiO_2 in gaseous photocatalysis, which include poor light adsorption, fast recombination of e^-–h^+ pairs, and inferior adsorptive capacity [20–24]. To achieve higher photocatalytic performance, most studies have focused on various modifications of TiO_2. To make TiO_2 possess a visible light response, Ce-doped TiO_2 and carbon quantum dot-decorated TiO_2 have been synthesized to enhance the light harvesting capacity [25,26]. To restrain the recombination of e^-–h^+ pairs, Ag@TiO_2 and TiO_2/TaS_2 composites have been synthesized to reduce the charge transfer resistance [27,28]. To improve the adsorptive capacity, nitrogen-doped graphene/TiO_2 and reduced graphene oxide/TiO_2 hybrids have been synthesized to strengthen gaseous pollutant adsorption [29,30]. These modifications indeed made TiO_2 a more efficient photocatalyst for the removal of gaseous o-xylene and acetaldehyde. However, these studies mostly focused on how to improve the photocatalytic performance of TiO_2 via material modification. However, for gas–solid photocatalysis, gaseous molecules adsorbed on the surface of a photocatalyst via physical and chemical adsorption is the first and essential step of photocatalytic reactions. Some reports have verified that the adsorptive effect of gaseous molecules on the TiO_2 surface can influence the band structure and active radicals of TiO_2, which has a considerable impact on the photocatalytic process [31–33]. For the photocatalysis of o-xylene and acetaldehyde, their adsorptive effect on the band structure and the active radicals of TiO_2 were generally ignored. Thus, the effect of o-xylene and acetaldehyde adsorption on TiO_2 has not been explored until now, and it deserves to be investigated in detail.

Owing to the distinct physical and chemical properties of different gaseous molecules, the TiO_2 surface with different adsorbed gaseous molecules will have different charge transfer situations [31]. Some gaseous molecules tend to donate their electrons to TiO_2 when adsorbed on the TiO_2 surface, which are called donor molecules. In contrast, some gaseous molecules tend to accept electrons from TiO_2 when adsorbed on the TiO_2 surface, which are called acceptor molecules. Electron transfer can induce an electric field [34–36], and corresponding band bending will form near the TiO_2 surface. For intrinsic TiO_2 (Scheme 1a), upward band bending can form when an acceptor molecule adsorbs on the TiO_2 surface (Scheme 1b). However, a donor molecule can result downward band bending (Scheme 1c) [31]. Regarding the direction of the band bending, if an electron is located at the formed electric field, as shown in Scheme 1b, the electron will tend to move to the bulk, and the band will bend upward. Oppositely, if an electron is located at the formed electric field, as shown in Scheme 1c, the electron will tend to move to the surface, and the band will bend downward. This upward or downward band bending will exert an effect on the separation of e^-–h^+ pairs and the generation of active radicals. Therefore, the interaction between TiO_2 and gaseous molecules should be given much attention and studied thoroughly.

However, real TiO_2 is not an intrinsic semiconductor but either a P- or N-type semiconductor. As shown in Scheme 2, for N-type TiO_2 (Scheme 2b, c), its E_F(bulk) will shift toward the conduction band. Then, electrons will flow from E_F(bulk) to E_F(surfasce) until an equilibrium occurs, which will induce upward band bending [31]. Thus, the band structure of N-type TiO_2 itself shows upward band bending. However, as shown in Schemes 2d and e, the band structure of P-type TiO_2 shows downward band bending.

Based on the aforementioned ideas, that is, that the interaction between TiO_2 and gaseous molecules deserves to be studied in depth and real TiO_2 is not an intrinsic semiconductor, in this study, rutile TiO_2 was synthesized through hydrolysis and calcination. The band bending of rutile TiO_2 induced by o-xylene and acetaldehyde adsorption was investigated, and its effect on the generation of active radicals was explored. The synthesized rutile TiO_2 was confirmed to be a P-type semiconductor. Furthermore, o-xylene was confirmed to be acceptor molecule, and acetaldehyde was a donor molecule according to theory and experiments. Rutile TiO_2 with different adsorbed molecules (o-xylene and acetaldehyde) had distinct band bending situations, and had distinct generation situations for active radicals. These results could explain the experimental phenomenon of why $\cdot O_2^-$ is the dominant radical for acetaldehyde photocatalysis, while o-xylene photocatalysis is dominant for ·OH. In this study, we not only investigated the interaction between TiO_2 and adsorbed gaseous molecules in depth but also expanded the insights to gaseous photocatalysis.

2. Experimental details

2.1. Chemical reagents

Tetrabutyl titanate (TBOT) and ethanol were supplied by Sinopharm Chemical Reagent Co. Ltd. DMPO (5,5-dimethyl-1-

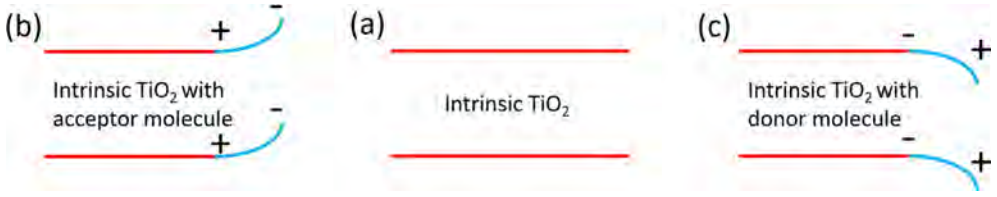

Scheme 1. Schematics of the band structure of (a) intrinsic TiO_2, (b) intrinsic TiO_2 with an acceptor molecule, and (c) intrinsic TiO_2 with a donor molecule.

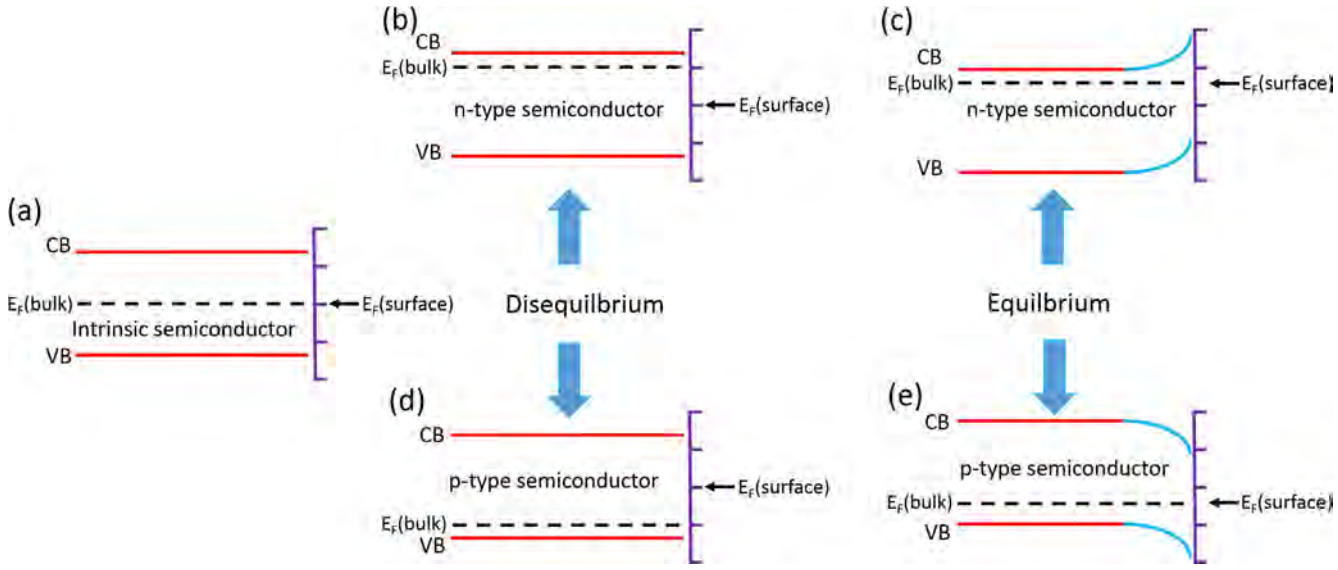

Scheme 2. Schematics of the band structures of (a) intrinsic TiO_2, (b) (c) N-type TiO_2, and (d) (e) P-type TiO_2.

pyrroline N-oxide, a radical scavenger) was supplied by DOJINDO Laboratories (purity > 99%). Then, 50-ppm o-xylene (50 ppm acetaldehyde) was supplied by Shanghai Wetry Standard Reference Gas Analytical Technology Co. Ltd. Deionized water (DI) was supplied by a Milli-Q system.

2.2. Synthesis of rutile TiO_2

First, 7 mL of DI was dispersed in 200 mL of ethanol by sonication for 10 min. Then, 10.5 mL of TBOT was slowly dropped in above the DI and ethanol mixture under magnetic stirring. The obtained suspension was centrifuged and washed with ethanol and DI three times (8000 rpm). Afterwards, the precipitates were dried in a vacuum oven at 40 °C for 10 h to obtain a powder sample. Finally, the powder sample was calcinated at 700 °C for 6 h, and rutile TiO_2 was obtained (Fig. S1). Mole numbers of all reagents used in the synthesis are listed in Table S1.

2.3. Characterizations

XRD spectra were collected on a X-ray diffractometer from a Bruker AXS GMBH (Germany). UV–Vis tests were conducted on a Lambda 950 spectrometer (PerkinElmer). Photoluminescence (PL) measurements were carried out on a luminescence instrument (LS-55) using an excited wavelength of 320 nm. Valence band X-ray photoelectron spectroscopy (XPS) was performed on a Microlab 310F. The adsorption of o-xylene and acetaldehyde on the TiO_2 surface was achieved using a PCA-1200 (a gas adsorption apparatus). Zeta potential tests were performed on a zetaPLUS instrument (Brookhaven Instruments). Electron spin resonance (ESR) measurements were performed on a JES-FA200 instrument by using DMPO as the radical scavenger. Mott–Schottky and photo-current tests were performed on a three electrode system (CHI 660D). Hall effect plots were made by using a physical property measurement system at 300 K (PPMS-9, Quantum Design).

2.4. Evaluation of photocatalytic activity

Gaseous o-xylene and acetaldehyde (concentration: 50 ppm, flow flux: 20 sccm) were used as the target pollutants to evaluate the photocatalytic performance. Gas chromatography (GC) was used to detect the concentrations of the target pollutants. The reaction chamber was a cuboid vessel sealed by a quartz pane (size of 15 cm × 8 cm × 1 cm). The powder sample was coated onto a glass slide for immobilization (size: 12 cm × 5 cm). The removal ratio (X) of the targeted pollutant was labeled as $X = (1 - C/C_0) \times 100\%$ in which C_0 was the initial concentration and C was the real-time concentration of the target pollutant (Irradiation: a 260-W fluorescent lamp, light wavelength: 400 nm, light intensity: 20 mW/cm^2).

2.5. Computational details

The first principle calculation was achieved using the Vienna Ab Initio Simulation (VASP) package. The geometries of the molecules in the gas and on the rutile TiO_2 (1 1 0) surface with different configurations were optimized by using generalized gradient approximation (GGA) implemented by Perdew–Burke–Erzhenhof (PBE). To account for the weak Van der Waal forces (vdW) between the gas molecules and the TiO_2 (1 1 0) surface, a vdW D correction method (DFT-D framework) provided by Grimme was used. The adsorption energy (ΔE_{ads}) was calculated according to Eq. (1):

$$\Delta E_{ads} = (E_{Molecule} + E_{Surface}) - E_{Molecule/Surface} \quad (1)$$

$E_{Molecule}$ represents the energy of a molecule in the gas phase, $E_{Surface}$ is the slab energy without adsorption, and $E_{Molecule/Surface}$ is the energy of the surface and molecular complex.

3. Results and discussion

3.1. Identification of the semiconductor type of the synthesized rutile TiO_2

First, the synthesized TiO_2 was characterized by XRD. As shown in Fig. S1, it was confirmed to be the rutile phase (JCPDS No. 21-1276). As mentioned in the Introduction, real TiO_2 itself is not an intrinsic semiconductor but has a downward or upward band bending structure, which depends on whether it is P or N type. Thus, it is necessary to know the semiconductor type of synthesized rutile TiO_2. As shown in Fig. 1a, rutile TiO_2 showed a negative slope in the Mott–Schottky plots, indicating that the synthesized TiO_2 was a P-type semiconductor [37,38]. Furthermore, the

enhancement direction of the photocurrent is a useful indicator to estimate the type of semiconductor. In general, a positive enhancement in the photocurrent usually occurs for an N-type semiconductor, while P-type semiconductor shows a negative enhancement in photocurrent [39–41]. As shown in Fig. 1b, the photocurrent of rutile TiO_2 showed an enhancement toward the negative direction with the illumination of light. This result verified that the synthesized TiO_2 was a P-type semiconductor. In addition, the Hall effect plots of rutile TiO_2 are displayed in Fig. 1c, and the curve shows a positive slope, which also means it is a P-type semiconductor [42]. Overall, the synthesized rutile TiO_2 was determined to be a P-type semiconductor, which was confirmed by three tests (Mott–Schottky plots, photocurrent response, and Hall effect plots). Thus, the band structure of rutile TiO_2 was clear. It had a downward band bending structure because of the P type semiconductor characteristic (Scheme 2e). However, to study the interaction of rutile TiO_2 with gaseous pollutants (o-xylene and acetaldehyde), another important aspect to know was the electron transfer properties of the gaseous pollutants (o-xylene and acetaldehyde).

3.2. Electron transfer properties of the gaseous pollutants (o-xylene and acetaldehyde)

To understand the electron transfer between TiO_2 and gaseous molecules, the most important thing to know is their detailed adsorption mode. The adsorption modes of o-xylene and acetaldehyde on the TiO_2 surface were investigated through theoretical computations. As shown in Fig. S1 (XRD spectrum), the strongest diffraction peak for rutile TiO_2 was for the (1 1 0) facet, which meant (1 1 0) was the main crystal facet of this studied TiO_2. Therefore, the theoretical computation was performed on the TiO_2 (1 1 0) facet with the corresponding gaseous molecule. The adsorption of o-xylene on the TiO_2 surface is shown in Fig. S2. There were five adsorption modes in total, which are labeled as O1, O2, O3, O4, and O5. The adsorption energies of O1–O5 were 0.1592, 0.0712, 0.0752, 0.01928, and 0.00127 eV, respectively. In general, the bigger the adsorption energy, the more stable the corresponding adsorption mode. Thus, type O1 was the most stable adsorption mode for o-xylene adsorption. Fig. S3 shows the adsorption mode of acetaldehyde on the TiO_2 surface. Six kinds of adsorption modes were observed, which are denoted as A1, A2, A3, A4, A5, and A6. The adsorption energies of A1–A6 were 0.686, 0.67, 0.616, 0.508, 0.462, and 0.32 eV, respectively. It was obvious that type A1 was the most stable adsorption mode for acetaldehyde adsorption. In summary, O1 and A1 were the most stable adsorption modes for o-xylene and acetaldehyde adsorption, respectively. Therefore, the charge density difference of O1 and A1 was computed to explore the electron transfer between TiO_2 and these gaseous molecules. The charge density difference for O1 is shown in Fig. 2a, while Fig. 2b shows the charge density difference for A1. In these two images, green is the electron-rich region, while yellow represents the electron-depleting region. For o-xylene adsorption (Fig. 2a), the green region mainly focused on the o-xylene molecule. Thus, the electrons tended to flow from TiO_2 to o-xylene, which meant o-xylene here was an acceptor molecule. In contrast, for acetaldehyde adsorption (Fig. 2b), the green region mainly centralized on TiO_2. Thus, in this case, acetaldehyde tended to donate its electrons to TiO_2 as a donor molecule. To summarize, in this case, o-xylene was confirmed to be an acceptor molecule, whereas acetaldehyde acted as a donor molecule, according to theoretical computations. In addition, these results are also in good agreement with some previous studies [43,44].

In addition to theoretical computations, zeta potential tests were conducted to explore the electron transfer of TiO_2 with different adsorbed molecules. Zeta potentials can reflect the electrical charge of the TiO_2 surface. Fig. 3a shows the zeta potential curve of bare TiO_2. As shown, TiO_2 has different zeta potential values at different pH. Here, TiO_2 with adsorbed acetaldehyde is labeled as TiO_2-ACE_{Ads}, and TiO_2 with adsorbed o-xylene is labeled as TiO_2-OXY_{Ads}. Fig. 3b shows the zeta potential curves for TiO_2, TiO_2-ACE_{Ads}, and TiO_2-OXY_{Ads} at a pH of 5.74. Clearly, the zeta potential of TiO_2 was approximately −31 mV for the three cyclic tests. However, TiO_2-ACE_{Ads} had a more positive zeta potential (approximately −18 mV) compared with that of TiO_2, and TiO_2-OXY_{Ads} had a more negative zeta potential (approximately −38 mV) compared with that of TiO_2. As mentioned in Scheme 1b, the acceptor molecule tended to accept the electrons of TiO_2 when it adsorbed onto the TiO_2 surface, and this made the TiO_2 surface more negatively charged. For the donor molecule, it tended to donate its electrons to TiO_2 when it adsorbed onto the TiO_2 surface, and this made the TiO_2 surface more positively charged (Scheme 1c). Thus, the results of the zeta potential tests verified that o-xylene was an acceptor molecule and acetaldehyde was a donor molecule. In summary, we confirmed both theoretically (Fig. 2) and experimentally (Fig. 3) that o-xylene acted as an acceptor molecule and acetaldehyde acted as a donor molecule.

3.3. Band bending of TiO_2 induced by o-xylene and acetaldehyde adsorption

Based on the aforementioned analyses, two critical problems were solved. One was that the synthesized rutile TiO_2 was a P-type semiconductor with a downward band bending structure. The second was that o-xylene acted as an acceptor molecule, while acetaldehyde acted as a donor molecule. Therefore, the interaction between TiO_2 and the gaseous molecules could be studied in detail. Acceptor molecules can induce upward band bending when adsorbed on the TiO_2 surface, whereas downward band bending would be generated if a donor molecule was adsorbed (Scheme 1).

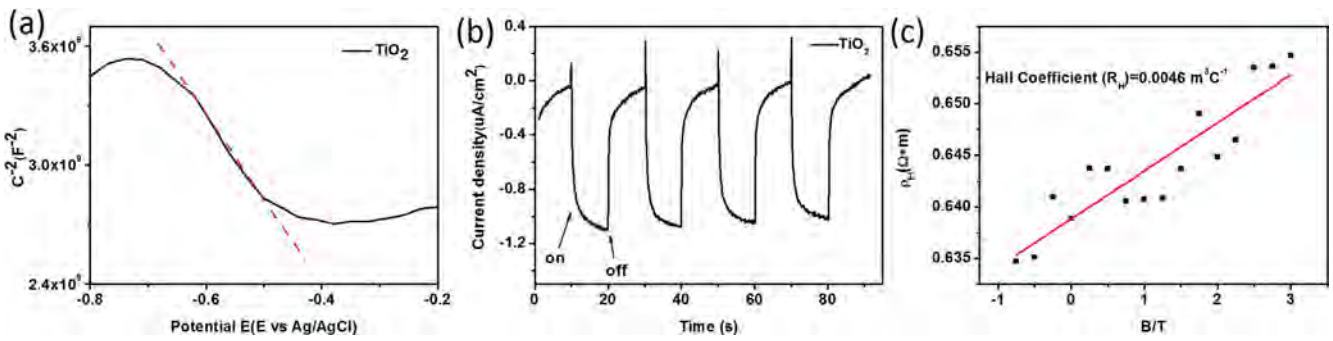

Fig. 1. (a) Mott–Schottky plots for rutile TiO_2, (b) photocurrent response for rutile TiO_2, and (c) Hall effect plots for rutile TiO_2.

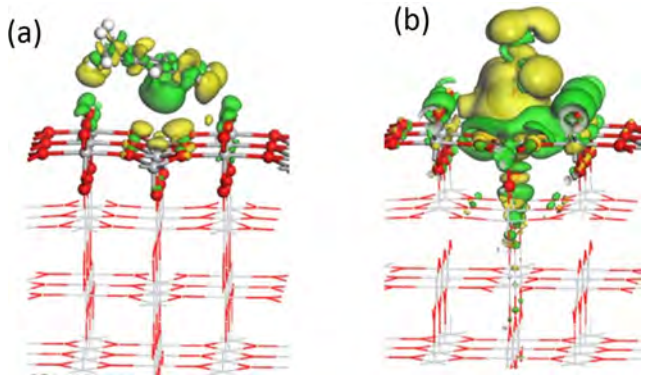

Fig. 2. Charge density differences for (a) O1 and (b) A1 (Green shows the electron-rich region, and yellow shows the electron-depleting region). (For interpretation of the references to colour in this figure legend, the reader is referred to the web version of this article.)

Thus, o-xylene adsorption can induce upward band bending of rutile TiO_2, and acetaldehyde adsorption can induce downward band bending of rutile TiO_2. As shown in Fig. 4a–c, acetaldehyde can donate its electrons to rutile TiO_2 because it is a donor molecule. Then, an electric field can form at the interface of rutile TiO_2 and acetaldehyde (Fig. 4c), and downward band bending can occur at the same time. Fig. 4a, d, and e show the charge transfer process between rutile TiO_2 and o-xylene. O-xylene acted as an acceptor molecule, and it can extract the electrons of rutile TiO_2. Thus, in contrast, the charge transfer at the interface of rutile TiO_2 and o-xylene (Fig. 4e) induced upward band bending.

Combining the fact that the rutile TiO_2 is a P-type semiconductor and that of acetaldehyde adsorption induced downward band bending, whereas o-xylene adsorption induced upward band bending, the band structure considering the interaction of TiO_2 and these gaseous molecules could be obtained. As shown in Fig. 5a, rutile TiO_2 had a downward band bending structure because it is P-type semiconductor. The extent of downward band bending of TiO_2-ACE_{Ads} would be strengthened owing to the positive effect of acetaldehyde (Fig. 5a–c). For TiO_2-OXY_{Ads}, the extent of its downward band bending was alleviated because of the negative effect of o-xylene (Fig. 5a, d and e). To confirm these band structure changes, some experimental evidence was required.

Photoluminescence (PL) spectroscopy is a nondestructive and contactless measurement that can be used to test band-bending changes [45,46]. The band-bending region in the near surface was approximately equal to the electric field region, which resulted from electron transfer of TiO_2 and the gaseous molecules [31]. The existence of this near surface electric field can facilitate the separation of photo-induced electron–hole pairs [32,33]. Thus, the recombination of the photo-induced electron–hole pairs in the band-bending region would be considerably depressed because of this electric field. Therefore, there was little PL emission coming from the band-bending region, and this region is called the dead layer, whereas the rest of the region of the band is called the active PL region. Thus, the change in the PL intensity could reflect the band structure change of TiO_2 with different adsorbed molecules. Based on the results shown in Fig. 5, it was verified that acetaldehyde adsorption strengthened the downward band bending of rutile TiO_2, and o-xylene adsorption alleviated it. Fig. 6a–c show the band structure of rutile TiO_2, TiO_2-OXY_{Ads} and TiO_2-ACE_{Ads}, respectively. Briefly, the length of the dead layer of TiO_2-OXY_{Ads} (Fig. 6b) was shorter compared with that of rutile TiO_2 (Fig. 6a). However, the length of the dead layer of TiO_2-ACE_{Ads} (Fig. 6c) was longer compared with that of TiO_2 (Fig. 6a). Oppositely, the active PL region of TiO_2-OXY_{Ads} was longer, whereas that of TiO_2-ACE_{Ads} was shorter in comparison to that of rutile TiO_2. Therefore, PL tests were conducted to evaluate the band structure change of TiO_2 with different adsorbed molecules. As shown in Fig. 7a, the PL intensity of TiO_2-ACE_{Ads} became weaker with increasing adsorption time compared with that of TiO_2, which meant acetaldehyde adsorption on the TiO_2 surface could shorten the active PL region. As shown in Fig. 7b, the PL intensity of TiO_2-OXY_{Ads} became stronger with increasing adsorption time compared with that of TiO_2, which meant o-xylene adsorption on the TiO_2 surface lengthened the active PL region. Thus, the PL results verified the effect of acetaldehyde and o-xylene on the band structure of TiO_2 experimentally (Fig. 5). In addition to PL tests, X-ray photoelectron spectroscopy (XPS) is also a common measurement used to evaluate the change in band structure [47–49]. Fig. 8a shows the valance band XPS spectra for TiO_2, TiO_2-OXY_{Ads}, and TiO_2-ACE_{Ads}, and Fig. 8b shows a partially enlarged spectra from that in Fig. 8a. As shown in Fig. 8b, the valance band positions of TiO_2, TiO_2-OXY_{Ads}, TiO_2-ACE_{Ads} were at 2.78 eV, 2.61 eV, and 2.96 eV (versus NHE = 0). Compared with TiO_2 (2.78 eV), TiO_2-OXY_{Ads} had a valence band position of 2.61 eV, which meant its valence band shifted upward. For TiO_2-ACE_{Ads}, it had a valance band position of 2.96 eV, which meant its valence band shifted downward. These results were in good agreement with those in Fig. 5. In summary, both PL and valence band XPS experimentally verified the effects of the gaseous molecules (o-xylene and acetaldehyde) on the band structure of TiO_2 (Fig. 5). Moreover, Fig. S4 shows the UV–Vis spectra of TiO_2, TiO_2-ACE_{Ads}-2h, and TiO_2-OXY_{Ads}-2h, and there was

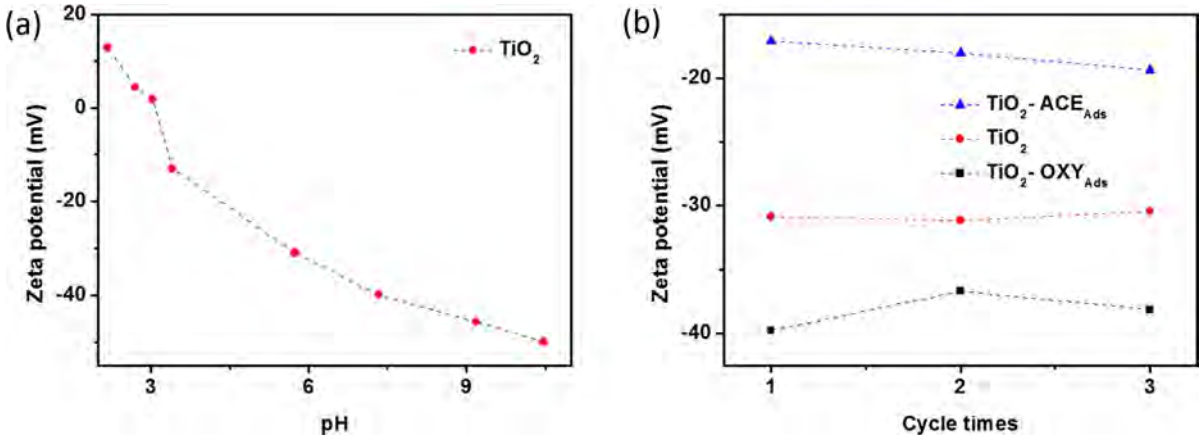

Fig. 3. (a) Zeta potential curve for TiO_2 as a function of different pH and (b) Zeta potential curves for TiO_2, TiO_2-ACE_{Ads}, and TiO_2-OXY_{Ads} at a pH of 5.74.

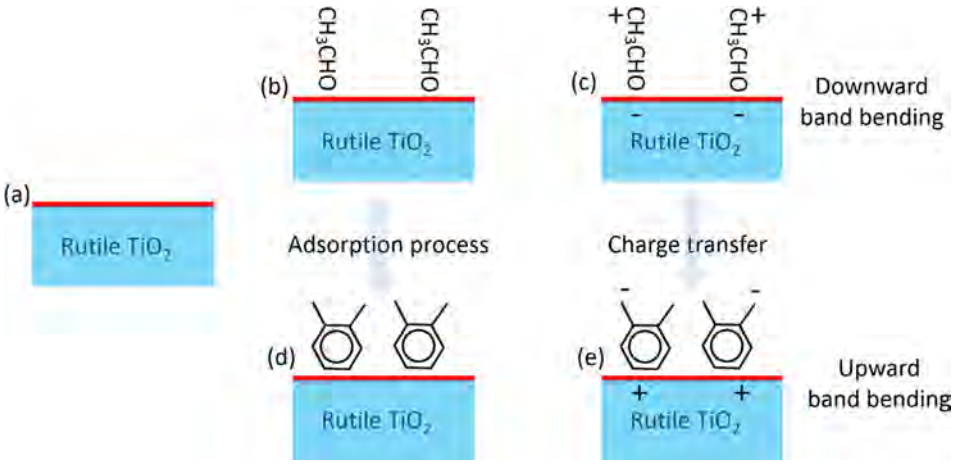

Fig. 4. (a)–(c) Charge transfer process for rutile TiO_2 with acetaldehyde and (a) (d),(e) charge transfer process for rutile TiO_2 with o-xylene.

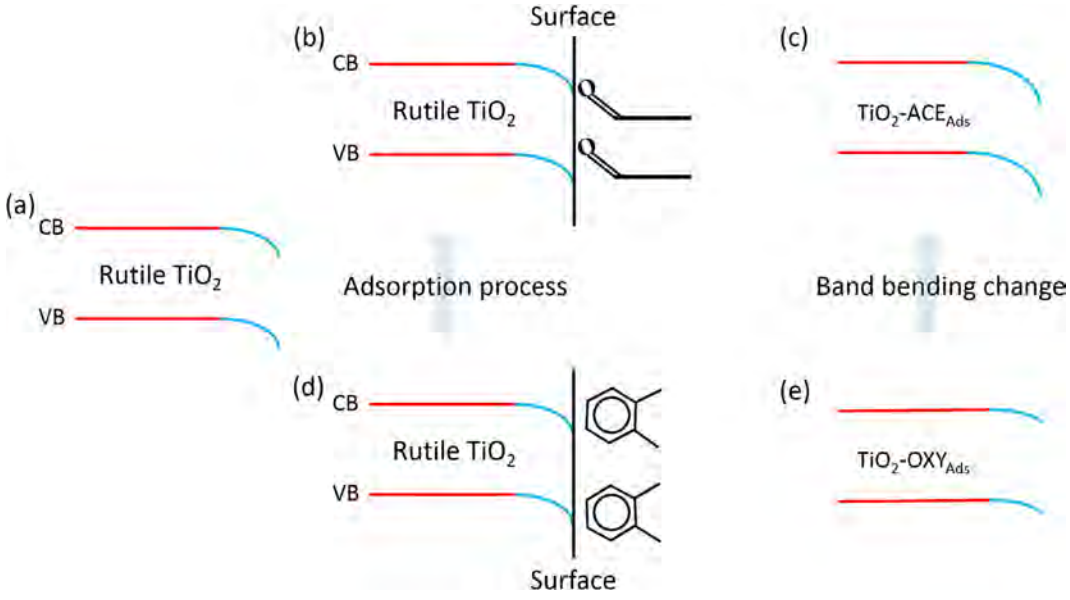

Fig. 5. (a)–(c) Band structure change from rutile TiO_2 to TiO_2-ACE_{Ads} and (a),(d),(e) band structure change from rutile TiO_2 to TiO_2-OXY_{Ads}.

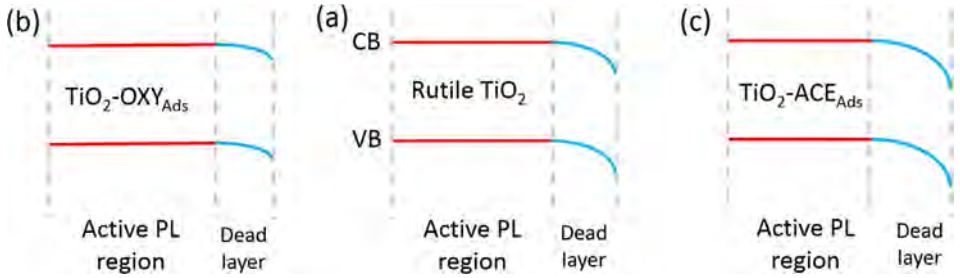

Fig. 6. (a) Band structure of rutile TiO_2, (b) TiO_2-OXY_{Ads}, and (c) TiO_2-ACE_{Ads}.

almost no difference in their UV–Vis spectra. Namely, band bending had no influence on the light adsorption.

3.4. Effects of o-xylene and acetaldehyde adsorption on active radical generation

A band structure change of TiO_2 induced by gaseous molecule adsorption will affect the generation of active radicals. It is well accepted that $\cdot O_2^-$ and $\cdot OH$ would be generated through the reaction of $O_2 + e^- \rightarrow \cdot O_2^-$ and $H_2O + h^+ \rightarrow \cdot OH + H^+$. Therefore, the probability of electrons and holes reaching the TiO_2 surface has a considerable influence on the generation of active radicals. Fig. 9 shows the corresponding energy barrier change of TiO_2 after gaseous molecule adsorption. Taking holes for example, the energy barrier of reaching the TiO_2 surface changed with different gaseous molecule adsorptions. As shown in Fig. 9b, owing to the alleviated down-

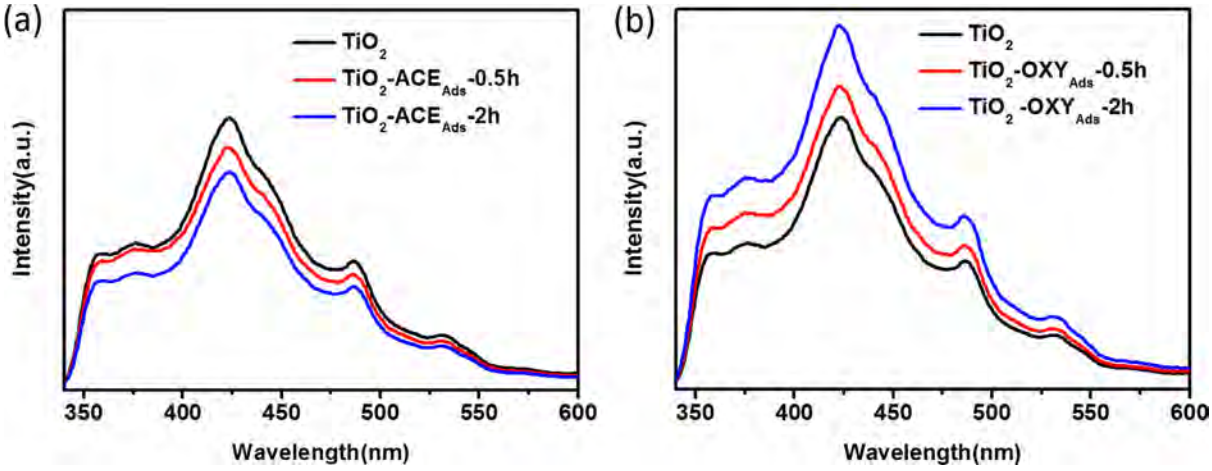

Fig. 7. (a) PL spectra of TiO_2, TiO_2-ACE_{Ads}-0.5 h, and TiO_2-ACE_{Ads}-2 h and (b) PL spectra of TiO_2, TiO_2-OXY_{Ads}-0.5 h, and TiO_2-OXY_{Ads}-2 h.

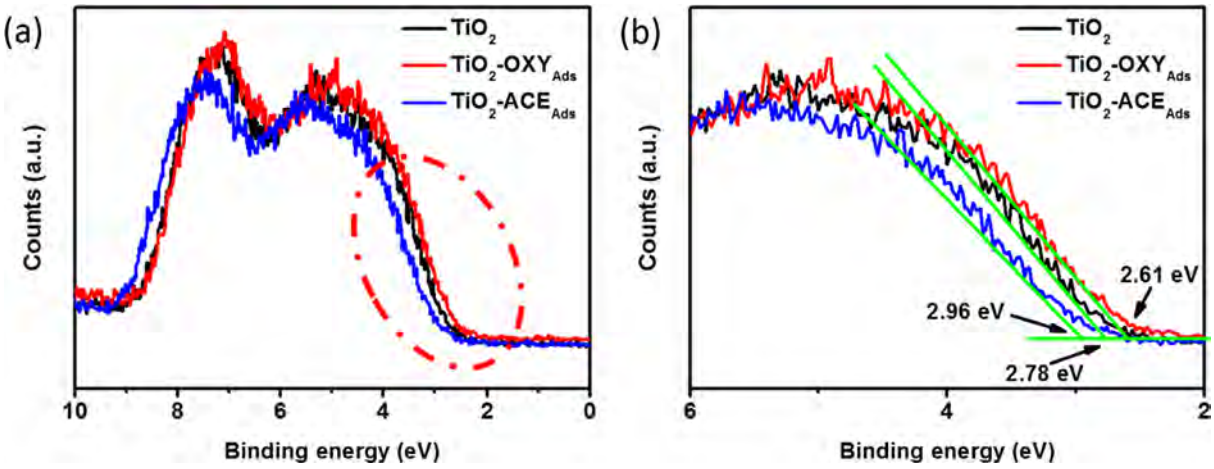

Fig. 8. (a) Valance band XPS spectra of TiO_2, TiO_2-ACE_{Ads} and TiO_2-OXY_{Ads} and (b) enlarged valence band XPS spectra of TiO_2, TiO_2-ACE_{Ads}, and TiO_2-OXY_{Ads}.

ward band bending, the energy barrier of holes of TiO_2-OXY_{Ads} decreased compared with that of TiO_2 (Fig. 9a). However, for TiO_2-ACE_{Ads} (Fig. 9c), it had a higher energy barrier for holes compared with TiO_2. Thus, TiO_2-OXY_{Ads} would generate more hydroxyl radicals (·OH), while TiO_2-ACE_{Ads} would generate less hydroxyl radicals in the photocatalysis process. For the generation of superoxide radicals ($\cdot O_2^-$), it should have the opposite generation situation to that of ·OH because the electric property of electrons is opposite to that of holes.

To monitor the generation of active radicals ($\cdot O_2^-$, ·OH), electron spin resonance (ESR) tests were conducted. As shown in Fig. 10a, there was little difference observed in the $\cdot O_2^-$ ESR signals of TiO_2, TiO_2-OXY_{Ads}, and TiO_2-ACE_{Ads}. This could be related to the probability of electrons reaching the TiO_2 surface. As shown in Fig. 9, the photo-induced electrons reaching the TiO_2 surface need not overcome any energy barrier. Thus, different band-bending situations (Fig. 9a–c) would not have a considerable effect on the process of electrons reaching the TiO_2 surface. Therefore, this could be responsible for the little difference observed in the $\cdot O_2^-$ ESR signals of three samples (Fig. 10a). Regarding the generation of ·OH, obvious differences were observed between TiO_2, TiO_2-OXY_{Ads}, and TiO_2-ACE_{Ads} (Fig. 10b). TiO_2-OXY_{Ads} had much stronger ·OH ESR signals compared with those of TiO_2, whereas the ·OH ESR intensity of TiO_2-ACE_{Ads} was much lower compared to that of TiO_2 (Fig. 10b). As is well known, the generation of ·OH is related to the probability of holes reaching the TiO_2 surface. As shown in

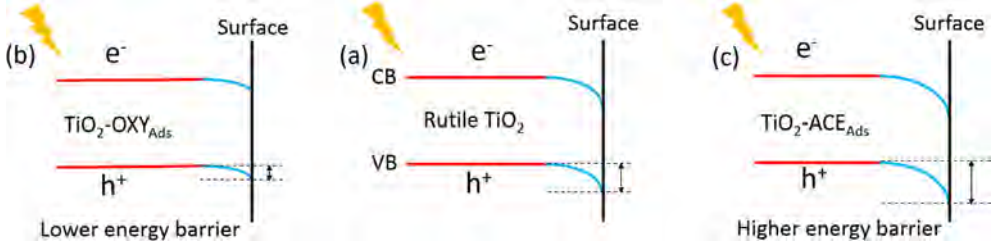

Fig. 9. (a) Schematics of the energy barriers of rutile TiO_2, (b) TiO_2-OXY_{Ads}, and (c) TiO_2-ACE_{Ads}.

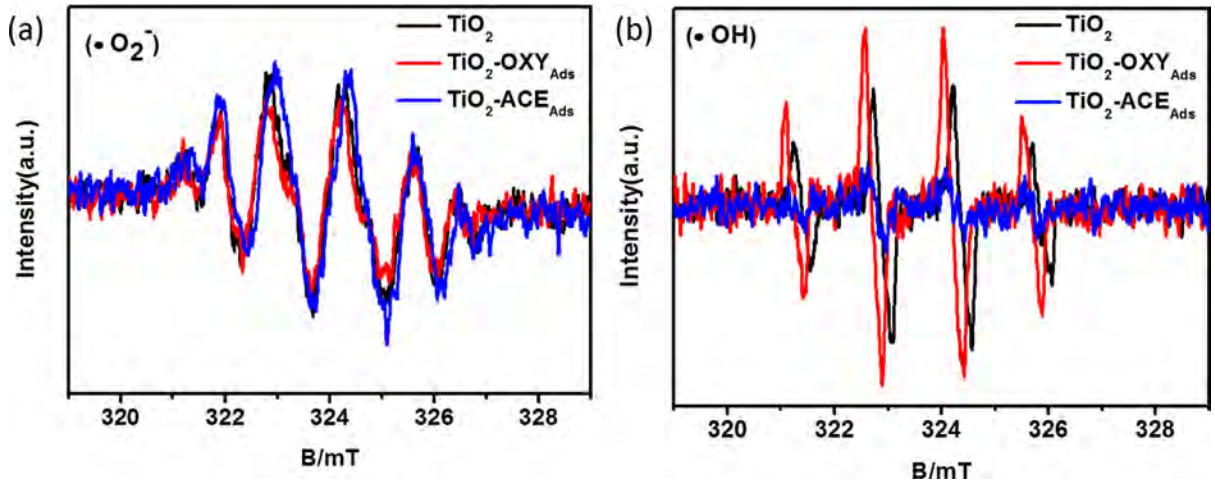

Fig. 10. (a) ESR signals of superoxide radicals ($\cdot O_2^-$) of TiO_2, TiO_2-OXY_{Ads}, and TiO_2-ACE_{Ads} (b) ESR signals of hydroxyl radicals ($\cdot OH$) of TiO_2, TiO_2-OXY_{Ads}, and TiO_2-ACE_{Ads}.

Fig. 9, the photo-induced holes reaching the TiO_2 surface need to overcome the energy barrier. As mentioned, owing to the alleviated downward band bending (Fig. 9b), the energy barrier of the holes of TiO_2-OXY_{Ads} became lower compared with that of TiO_2 (Fig. 9a). However, for TiO_2-ACE_{Ads} (Fig. 9c), it had a higher energy barrier for holes compared to that of TiO_2 (Fig. 9a). Thus, TiO_2-OXY_{Ads} tended to generate more $\cdot OH$, whereas TiO_2-ACE_{Ads} tended to generate less $\cdot OH$ compared with TiO_2. This was in good agreement with the results of the $\cdot OH$ ESR tests (Fig. 10b). In summary, different band-bending situations (Fig. 9) can affect the probability of electrons and holes reaching the TiO_2 surface. To reach the TiO_2 surface, holes need to overcome an energy barrier, whereas electrons do not. Therefore, the generation of $\cdot OH$ was influenced considerably, whereas the generation of $\cdot O_2^-$ was influenced slightly, and this was verified by the ESR tests (Fig. 10).

To investigate the roles of active radicals ($\cdot O_2^-$, $\cdot OH$) in the photodegradation of o-xylene and acetaldehyde, controlled atmosphere experiments were carried out. As shown in Fig. 11, there were three different atmospheric conditions. The $N_2 + O_2 + H_2O$ atmosphere ensured that both $\cdot O_2^-$ and $\cdot OH$ were generated and effective in the photocatalysis process. Similarly, the $N_2 + O_2$ atmosphere ensured that only $\cdot O_2^-$ was generated and effective, while the $N_2 + H_2O$ atmosphere ensured that only $\cdot OH$ was generated and effective. As shown in Fig. 11a, for the photodegradation of o-xylene, $\cdot OH$ played the predominant role ($N_2 + H_2O$), and $\cdot O_2^-$ played the secondary role ($N_2 + O_2$). In contrast, for the photodegradation of acetaldehyde (Fig. 11b), the predominant radical was $\cdot O_2^-$ ($N_2 + O_2$), whereas the secondary radical was $\cdot OH$ ($N_2 + H_2O$). These results could be well explained by the aforementioned band structure changes (Fig. 9) and radical generation situations (Fig. 10). In summary, the interaction between TiO_2 and the gaseous molecules was verified, and the effect of gaseous molecule adsorption (o-xylene and acetaldehyde) on the photocatalysis was verified. Furthermore, to confirm the universality, ZnO with different adsorbed gaseous molecules was selected for ESR tests. As shown in Figs. S5, 6, for ZnO with adsorbed o-xylene and acetaldehyde, the generation of $\cdot OH$ was influenced considerably, while the generation of $\cdot O_2^-$ was influenced only slightly, which was in agreement with the results for TiO_2. This indicates that the adsorbed molecules had an influence not only on the generation of radicals from TiO_2 but also on that of another semiconductor (ZnO).

Briefly, compared with literature studies that have focused on the synthesis of efficient photocatalysts [25–30], there were two main novel parts of this study. First, the effect of o-xylene and acetaldehyde adsorption on the band structure of TiO_2 was taken into account and investigated. Thus, more attention can be given to the interaction itself between photocatalysts and VOCs in the future. However, the change in band bending induced by o-xylene and acetaldehyde adsorption had a considerable impact on the generation of active radicals ($\cdot O_2^-$, $\cdot OH$). This can provide

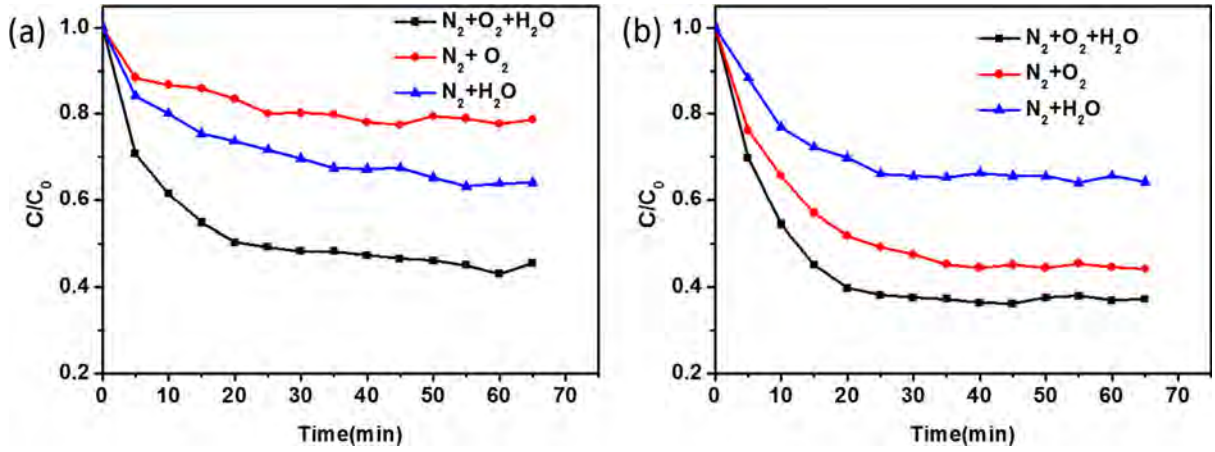

Fig. 11. (a) Photodegradation of o-xylene by TiO_2 under different controlled atmospheres and (b) photodegradation of acetaldehyde by TiO_2 under different controlled atmospheres.

new insights into the design and optimization of the band structures of photocatalysts.

4. Conclusions

In summary, the effect of electron transfer between TiO_2 and adsorbed molecules on band structure was taken into account. The synthesized rutile TiO_2 itself had a downward band bending structure. O-xylene was confirmed to act as an acceptor molecule, and acetaldehyde was confirmed to be a donor molecule both theoretically (Charge density difference) and experimentally (zeta potential tests). O-xylene adsorption alleviated the downward band bending of TiO_2, whereas acetaldehyde adsorption strengthened the downward band bending of TiO_2, which was verified experimentally by PL and valence band XPS measurements. Thus, more attention should be given to the interaction between photocatalysts and VOCs in the future. The change of band bending induced by o-xylene and acetaldehyde adsorption had a considerable impact on the generation of active radicals ($\cdot O_2^-$, $\cdot OH$). As a result, the generation of $\cdot OH$ was influenced considerably, whereas the generation of $\cdot O_2^-$ was influenced slightly, which was confirmed by ESR tests. These results could well explain the experimental phenomenon that $\cdot O_2^-$ is the dominant radical for acetaldehyde photocatalysis and $\cdot OH$ is the dominant radical for o-xylene photocatalysis. This provides new insights into the design and optimization of the band structures of photocatalysts. Briefly, this work not only investigated the interaction between TiO_2 and adsorbed gaseous molecules in depth but also expanded insight into gaseous photocatalysis.

CRediT authorship contribution statement

Qinglong Zeng: Data curation, Software, Writing - original draft. **Xiao Wang:** Investigation. **Xiaofeng Xie:** Writing - review & editing, Project administration, Supervision. **Asad Mahmood:** Software. **Guanhong Lu:** Methodology. **Yan Wang:** Writing - review & editing. **Jing Sun:** Writing - review & editing, Methodology, Supervision.

Declaration of Competing Interest

The authors declare that they have no known competing financial interests or personal relationships that could have appeared to influence the work reported in this paper.

Acknowledgements

This work was financially supported by the National Key Research and Development Program of China (2016YFA0203000), Shanghai "Belt and Road" Program for Young Foreign Scientists (17520742600), NSFC-DFG bilateral organization program (51761135107), and Shanghai Sailing Program (18YF1426800).

Appendix A. Supplementary material

Supplementary data to this article can be found online at https://doi.org/10.1016/j.jcis.2020.03.114.

References

[1] Q. Zhang, S. Yuan, B. Xu, Y. Xu, K. Cao, Z. Jin, C. Qiu, M. Zhang, C. Su, T. Ohno, A facile approach to build $Bi2O_2CO_3$/PCN nanohybrid photocatalysts for gaseous acetaldehyde efficient removal, Catal. Today 315 (2018) 184–193.
[2] Q. Zeng, X. Xie, X. Wang, G. Lu, H. Li, S. Cheng Lee, J. Sun, New insights into the synergistic effect of active radicals and adsorptive ability on the photodegradation of gaseous acetaldehyde over reduced graphene Oxide/P25 composite, J. Hazard. Mater. 380 (2019) 120814.
[3] Y. Wu, S. Shi, S. Yuan, T. Bai, S. Xing, Insight into the enhanced activity of Ag/NiOx-MnO_2 for catalytic oxidation of o-xylene at low temperatures, Appl. Surf. Sci. 479 (2019) 1262–1269.
[4] Y. Wang, C. Zhang, H. He, Insight into the role of Pd state on Pd-based catalysts in o-xylene oxidation at low temperature, ChemCatChem 10 (5) (2018) 998–1004.
[5] G. Muthuraman, M. Thirumavalavan, M. Il Shik, In situ electrochemically generated peroxymonophosphoric acid as an oxidant for the effective removal of gaseous acetaldehyde, Chem. Eng. J. 325 (2017) 449–456.
[6] L. Liu, J. Li, H. Zhang, L. Li, P. Zhou, X. Meng, M. Guo, J. Jia, T. Sun, In situ fabrication of highly active gamma-MnO_2/$SmMnO_3$ catalyst for deep catalytic oxidation of gaseous benzene, ethylbenzene, toluene, and o-xylene, J. Hazard. Mater. 362 (2019) 178–186.
[7] Z. Zhu, B. Wang, Q. Yao, Y. Zhou, H. Yang, Y. Liu, $H_3PW_{12}O_{40}$/mpg-C_3N_4 as an efficient and reusable catalyst in the alkylation of o-xylene and styrene, Appl. Org. Chem. 33 (10) (2019).
[8] P.A. Pepin, J.D. Lee, C.B. Murray, J.M. Vohs, Thermal and photocatalytic reactions of methanol and acetaldehyde on Pt-modified brookite TiO_2 nanorods, ACS Catal. 8 (12) (2018) 11834–11846.
[9] A. Mahmood, X. Wang, G. Shi, Z. Wang, X. Xie, J. Sun, Revealing adsorption and the photodegradation mechanism of gas phase o-xylene on carbon quantum dots modified TiO_2 nanoparticles, J. Hazard. Mater. 386 (2020) 121962.
[10] J. Billet, S. Vandewalle, M. Meire, N. Blommaerts, P. Lommens, S.W. Verbruggen, K. De Buysser, F. Du Prez, I. Van Driessche, Mesoporous TiO_2 from poly(N, N-dimethylacrylamide)-b-polystyrene block copolymers for long-term acetaldehyde photodegradation, J. Mater. Sci. 55 (5) (2019) 1933–1945.
[11] H.E. Dan-Nong, Y.A.N. Liang, D. Ya-Mei, T. Qin, High-efficient synthesis and photocatalytic properties of Ag/AgBr/TiO_2 monolithic photocatalysts using sodium alginate as substrate, J. Inorg. Mater. 32 (6) (2017) 637.
[12] C.U.I. Xiao-Li, L.I. Hui, L.I. Zhong, M.A. Xiao-Qing, C. Yang, S.U.N. Tong, Facile synthesis of visible light activated carbon-incorporated Mn doped TiO_2 microspheres via flame thermal method, J. Inorg. Mater. 30 (9) (2015) 1002.
[13] X. Chen, J. Wei, R. Hou, Y. Liang, Z. Xie, Y. Zhu, X. Zhang, H. Wang, Growth of g-C_3N_4 on mesoporous TiO_2 spheres with high photocatalytic activity under visible light irradiation, Appl. Catal. B: Environ. 188 (2016) 342–350.
[14] Y. Chen, D. Chen, J. Chen, Q. Lu, M. Zhang, B. Liu, Q. Wang, Z. Wang, Facile synthesis of Bi nanoparticle modified TiO_2 with enhanced visible light photocatalytic activity, J. Alloys Compd. 651 (2015) 114–120.
[15] H. Cui, W. Zhao, C. Yang, H. Yin, T. Lin, Y. Shan, Y. Xie, H. Gu, F. Huang, Black TiO_2 nanotube arrays for high-efficiency photoelectrochemical water-splitting, J. Mater. Chem. A 2 (23) (2014) 8612.
[16] J. Du, Z. Wang, G. Zhao, Y. Qian, H. Chen, J. Yang, X. Liu, K. Li, C. He, W. Du, I. Shakir, Facile synthesis and enhanced photocatalytic activity of porous Sn/Nd-codoped TiO_2 monoliths, Micropor. Mesopor. Mater. 195 (2014) 167–173.
[17] F. Zhang, M. Wang, X. Zhu, B. Hong, W. Wang, Z. Qi, W. Xie, J. Ding, J. Bao, S. Sun, C. Gao, Effect of surface modification with H_2S and NH_3 on TiO_2 for adsorption and photocatalytic degradation of gaseous toluene, Appl. Catal. B: Environ. 170–171 (2015) 215–224.
[18] F. Yang, G. Han, D. Fu, Y. Chang, H. Wang, Improved photodegradation activity of TiO_2 via decoration with SnS_2 nanoparticles, Mater. Chem. Phys. 140 (1) (2013) 398–404.
[19] Z. Wang, Y. Huang, W. Ho, J. Cao, Z. Shen, S.C. Lee, Fabrication of $Bi_2O_2CO_3$/g-C_3N_4 heterojunctions for efficiently photocatalytic NO in air removal: in-situ self-sacrificial synthesis, characterizations and mechanistic study, Appl. Catal. B: Environ. 199 (2016) 123–133.
[20] F. Teng, M. Li, C. Gao, G. Zhang, P. Zhang, Y. Wang, L. Chen, E. Xie, Preparation of black TiO_2 by hydrogen plasma assisted chemical vapor deposition and its photocatalytic activity, Appl. Catal. B: Environ. 148–149 (2014) 339–343.
[21] P. Sun, R. Xue, W. Zhang, I. Zada, Q. Liu, J. Gu, H. Su, Z. Zhang, J. Zhang, D. Zhang, Photocatalyst of organic pollutants decomposition: TiO_2/glass fiber cloth composites, Catal. Today 274 (2016) 2–7.
[22] R.M. Mohamed, E.S. Aazam, Effect of Sn loading on the photocatalytic aniline synthesis activity of TiO_2 nanospheres, J. Alloys Compd. 595 (2014) 8–13.
[23] K. Lv, X. Guo, X. Wu, Q. Li, W. Ho, M. Li, H. Ye, D. Du, Photocatalytic selective oxidation of phenol to produce dihydroxybenzenes in a TiO_2/UV system: hydroxyl radical versus hole, Appl. Catal. B: Environ. 199 (2016) 405–411.
[24] Y. Li, K. Lv, W. Ho, F. Dong, X. Wu, Y. Xia, Hybridization of rutile TiO2 ($rTiO_2$) with g-C_3N_4 quantum dots (CN QDs): an efficient visible-light-driven Z-scheme hybridized photocatalyst, Appl. Catal. B: Environ. 202 (2017) 611–619.
[25] J.Y. Lee, J.H. Choi, Sonochemical synthesis of ce-doped TiO_2 nanostructure: a visible-light-driven photocatalyst for degradation of toluene and O-xylene, Materials (Basel) 12 (8) (2019).
[26] Y. Hu, X. Xie, X. Wang, Y. Wang, Y. Zeng, D.Y.H. Pui, J. Sun, Visible-light upconversion carbon quantum dots decorated TiO_2 for the photodegradation of flowing gaseous acetaldehyde, Appl. Surf. Sci. 440 (2018) 266–274.
[27] Q. Zeng, X. Xie, X. Wang, Y. Wang, G. Lu, D.Y.H. Pui, J. Sun, Enhanced photocatalytic performance of Ag@TiO_2 for the gaseous acetaldehyde photodegradation under fluorescent lamp, Chem. Eng. J. 341 (2018) 83–92.
[28] Q. Zeng, X. Wang, X. Xie, G. Lu, Y. Wang, S. Cheng Lee, J. Sun, TiO_2/TaS_2 with superior charge separation and adsorptive capacity to the photodegradation of gaseous acetaldehyde, Chem. Eng. J. 379 (2020) 122395.
[29] W. Lin, X. Xie, X. Wang, Y. Wang, D. Segets, J. Sun, Efficient adsorption and sustainable degradation of gaseous acetaldehyde and o-xylene using rGO-TiO_2 photocatalyst, Chem. Eng. J. 349 (2018) 708–718.

[30] X. Dai, Y. Wang, X. Wang, S. Tong, X. Xie, Polarity on adsorption and photocatalytic performances of N-GR/TiO_2 towards gaseous acetaldehyde and ethylene, Appl. Surf. Sci. 485 (2019) 255–265.
[31] Z. Zhang, J.T. Yates Jr., Band bending in semiconductors: chemical and physical consequences at surfaces and interfaces, Chem. Rev. 112 (10) (2012) 5520–5551.
[32] S. Ma, Z. Zhang, I. Harrison, Photoreduction of hydrogen cations on TiO_2 and its impact on surface band bending and the charge carrier recombination rate: a photoluminescence study under high vacuum conditions, J. Phys. Chem. C 122 (15) (2018) 8288–8294.
[33] S. Ma, M.E. Reish, Z. Zhang, I. Harrison, J.T. Yates, Anatase-selective photoluminescence spectroscopy of P25 TiO_2 nanoparticles: different effects of oxygen adsorption on the band bending of anatase, J. Phys. Chem. C 121 (2) (2017) 1263–1271.
[34] K. Ozawa, M. Emori, S. Yamamoto, R. Yukawa, S. Yamamoto, R. Hobara, K. Fujikawa, H. Sakama, I. Matsuda, Electron-hole recombination time at TiO_2 single-crystal surfaces: influence of surface band bending, J. Phys. Chem. Lett. 5 (11) (2014) 1953–1957.
[35] M.T. Uddin, Y. Nicolas, C. Olivier, T. Toupance, M.M. Müller, H.-J. Kleebe, K. Rachut, J. Ziegler, A. Klein, W. Jaegermann, Preparation of RuO_2/TiO_2 mesoporous heterostructures and rationalization of their enhanced photocatalytic properties by band alignment investigations, J. Phys. Chem. C 117 (42) (2013) 22098–22110.
[36] F.S. Roberts, S.L. Anderson, A.C. Reber, S.N. Khanna, Initial and final state effects in the ultraviolet and X-ray photoelectron spectroscopy (UPS and XPS) of size-selected Pdn clusters supported on TiO_2(110), J. Phys. Chem. C 119 (11) (2015) 6033–6046.
[37] B. Sun, W. Zhou, H. Li, L. Ren, P. Qiao, F. Xiao, L. Wang, B. Jiang, H. Fu, Magnetic Fe_2O_3/mesoporous black TiO_2 hollow sphere heterojunctions with wide-spectrum response and magnetic separation, Appl. Catal. B: Environ. 221 (2018) 235–242.
[38] S. Fujimoto, H. Tsuchiya, Semiconductor properties and protective role of passive films of iron base alloys, Corros. Sci. 49 (1) (2007) 195–202.
[39] W. Guo, J. Zhang, G. Li, C. Xu, Enhanced photocatalytic activity of P-type (K, Fe) co-doped g-C_3N_4 synthesized in self-generated NH_3 atmosphere, Appl. Surf. Sci. 470 (2019) 99–106.
[40] J. Luo, G. Dong, Y. Zhu, Z. Yang, C. Wang, Switching of semiconducting behavior from n -type to p -type induced high photocatalytic NO removal activity in g-C_3N_4, Appl. Catal. B: Environ. 214 (2017) 46–56.
[41] L. Zhang, J. Qu, T. Yu, Y. Chen, W. Pang, M. Qu, H. Wang, Y. Zhang, H. Yan, Control of the structure and photoelectrical properties of Cu(InGa)Se_2 film by Ga deposition potential in two-step electrodeposition, J. Mater. Sci.: Mater. Electron. 29 (23) (2018) 20104–20112.
[42] J.J.J. Vijila, K. Mohanraj, G. Sivakumar, Photovoltaic p-n structure of $MoSb_2-xCuxSe_4$/CdS absorber films obtained via chemical bath deposition, Mater. Res. Express 3 (7) (2016) 076408.
[43] Y. Zhi, S. Ma, H. Xia, Y. Zhang, Z. Shi, Y. Mu, X. Liu, Construction of donor-acceptor type conjugated microporous polymers: a fascinating strategy for the development of efficient heterogeneous photocatalysts in organic synthesis, Appl. Catal. B: Environ. 244 (2019) 36–44.
[44] A. Vargas, G. Santarossa, A. Baiker, Ab initio molecular dynamics investigation of the coadsorption of acetaldehyde and hydrogen on a platinum nanocluster, J. Phys. Chem. C 115 (21) (2011) 10661–10667.
[45] A. Stevanovic, M. Buttner, Z. Zhang, J.T. Yates Jr., Photoluminescence of TiO_2: effect of UV light and adsorbed molecules on surface band structure, J. Am. Chem. Soc. 134 (1) (2012) 324–332.
[46] T.H. Gfroerer, Photoluminescence in Analysis of Surfaces and Interfaces, 2006.
[47] H. Tan, Z. Zhao, M. Niu, C. Mao, D. Cao, D. Cheng, P. Feng, Z. Sun, A facile and versatile method for preparation of colored TiO_2 with enhanced solar-driven photocatalytic activity, Nanoscale 6 (17) (2014) 10216–10223.
[48] X. Liu, L. Chen, Q. Liu, J. He, K. Li, W. Yu, J.-P. Ao, K.-W. Ang, Band alignment of atomic layer deposited TiO_2/multilayer MoS_2 interface determined by x-ray photoelectron spectroscopy, J. Alloys Compd. 698 (2017) 141–146.
[49] R.S. Ajimsha, A.K. Das, V.K. Sahu, M.P. Joshi, L.M. Kukreja, U.P. Deshpande, T. Shripathi, Valance band offset of TiO_2/$CuGaO_2$ hetero-structure measured by x-ray photoelectron spectroscopy, Sol. Energy Mater. Sol. Cells 140 (2015) 446–449.